Reactivity of Monolayer-Protected Gold Cluster Molecules: Steric Effects

Allen C. Templeton, Michael J. Hostetler, Cynthia T. Kraft, and Royce W. Murray*

Contribution from the Kenan Laboratories of Chemistry, University of North Carolina, Chapel Hill, North Carolina 27599-3290

Received November 10, 1997

Abstract: The steric environment of alkanethiolate ligand shells of monolayer-protected gold cluster (MPCs) molecules has been investigated in three ways. First, the S_N2 reactivity of ω-bromoalkanethiolate-functionalized MPCs with primary amines has been shown to respond to the steric bulk of the incoming nucleophile (rates of *n*-propylamine> isopropylamine> *tert*-butylamine), and to the relative chain lengths of ω-bromoalkanethiolate and surrounding alkanethiolate chains (rates of C12:C12Br > C12:C8Br > C12:C3Br). Also, unlike 2D-SAMs, ω-bromo-functionalized MPCs and primary alkyl halide monomers (RBr) have comparable S_N2 reactivities. These results are significant in that little previously was known about the chemical reactivities of the monolayers on MPCs, and in that the poly-functional ω-bromoalkanethiolate MPCs are shown to be highly reactive, i.e., as many as 20 S_N2 displacements occur per cluster molecule. Second, steric aspects of alkanethiolate monolayers on Au clusters are shown to affect the rate of cyanide-mediated decomposition of the gold core, which slows with increased chain length (up to C10) and steric bulk. Third, solution infrared spectroscopy demonstrates that, in nonpolar solvents, the alkanethiolate ligands on Au MPCs have a disorder approaching that of liquid alkanes. These results support a model of MPC ligand environment of decreasing chain packing density as the distance from the gold core increases, a motif that likely arises from the high curvature of gold nanoparticle surfaces.

Recent synthetic progress in metallic and semiconducting nanoparticles[1,2] has been stimulated by their potential for displaying unusual properties, including those associated with dimensions intermediate between those of small metal complexes and bulk systems.[3−5] Our own laboratory, for example, has shown[6] that alkanethiolate monolayer-protected gold clusters (MPCs) display solution-phase ensemble Coulomb staircase behavior, with step-spacing a function of nanoparticle size.[7] Alkanethiolate/gold MPCs seem particularly well-suited for probing nanoscale physical properties as a function of metal core dimension and chain length of the alkanethiolate ligand.[8] Besides ease of synthesis,[9] these MPCs behave as robust large molecules and are amenable to characterization by a variety of analytical methods.[10]

While we and others have explored[6−20] the synthesis and properties of alkanethiolate-stabilized Au clusters, and clusters have been produced with ω-functionalized monolayers, including electroactive ones,[14−16] the literature is largely silent on the

(1) (a) Schmid, G. *Clusters and Colloids. From Theory to Applications*; VCH: New York, 1994. (b) Matijevic, E. *Curr. Opin. Coll. Interface Sci*. **1996**, *1*, 176. (c) Belloni, J. *Curr. Opin. Coll. Interface Sci*. **1996**, *1*, 184. (d) Klabunde, K. J.; Stark, J.; Koper, O.; Mohs, C.; Park, D. G.; Decker, S.; Jiang, Y.; Lagadic, I.; Zhang, D. *J. Phys. Chem*. **1996**, *100*, 12142. (e) Haberland, H., Ed. *Clusters of Atoms and Molecules*; Springer-Verlag: New York, 1994. (f) Heinglein, A. *Ber. Bunsen-Ges. Phys. Chem*. **1995**, *99*, 903. (g) Schmid, G. *Chem. Rev*. **1992**, *92*, 1709. (h) Fendler, J. H.; Meldrum, F. C. *Adv. Mater*. **1995**, *7*, 607. (i) Schmid, G.; Maihack, V.; Lantermann, F.; Peschel, S. *J. Chem. Soc., Dalton Trans*. **1996**, 589.

(2) (a) Alivisatos, A. P. *Science* **1996**, *271*, 933. (b) Weller, H. *Angew. Chem., Int. Ed. Engl.* **1993**, *32*, 41. (c) Murray, C. B.; Kagan, C. R.; Bawendi, M. G. *Science* **1995**, *270*, 1335. (d) Guzelian, A. A.; Katari, J. E. B.; Kadavanich, A. V.; Banin, U.; Hamad, K.; Juban, E.; Alivisatos, A. P.; Wolters, R. H.; Arnold, C. C.; Heath, J. R. *J. Phys. Chem*. **1996**, *100*, 7212. (e) Ahmadi, T. S.; Wang, Z. L.; Henglein, A.; El-Sayed, M. A. *Chem. Mater*. **1996**, *8*, 1161. (f) Ahmadi, T. S.; Wang, Z. L.; Green, T. C.; Henglein, A.; El-Sayed, M. A. *Science* **1996**, *272*, 1924. (g) Harfenist, S. A.; Wang, Z. L.; Alvarez, M. M.; Vezmar, I.; Whetten, R. L. *J. Phys. Chem*. **1996**, *100*, 13904.

(3) Bawendi, M.; Stiegerwald, M. L.; Brus, L. E. *Annu. Rev. Phys. Chem*. **1990**, *4*, 477.

(4) Wang, Y.; Herron, N. J. *J. Phys. Chem*. **1991**, *95*, 525.

(5) Siegel, R. *Nanostruct. Mater*. **1993**, *3*, 1.

(6) Ingram, R. S.; Hostetler, M. J.; Murray, R. W.; Schaaf, T. G.; Khoury, J. T.; Whetten, R. L.; Bigioni, T. P.; Guthrie, D. K.; First, P. N. *J. Am. Chem. Soc.* **1997**, *119*, 9279.

(7) (a) Ingram, R. S. Ph.D. Dissertation, University of North Carolina at Chapel Hill, Chapel Hill, 1997. (b) Chen, S.; Ingram, R. S.; Hostetler, M. J.; Pietron, J. J.; Murray, R. W.; Schaaff, T. G.; Khoury, J. T.; Alvarez, M. M.; Whetten, R. L. Manuscript in preparation.

(8) (a) Leff, D. V.; Ohara, P. C.; Heath, J. R.; Gelbart, W. M. *J. Phys. Chem*. **1995**, *99*, 7036. (b) Motte, L.; Billoudet, F.; Pileni, M. P. *J. Phys. Chem*. **1995**, *99*, 16425.

(9) Brust, M.; Walker, M.; Bethell, D.; Schriffrin, D. J.; Whyman, R. *J. Chem. Soc., Chem. Commun*. **1994**, 801.

(10) Hostetler, M. J.; Murray, R. W. *Curr. Opin. Coll. Interface Sci*. **1997**, *2*, 42, and references therein.

(11) Terrill, R. H.; Postlewaithe, T. A.; Chen, C.-H.; Poon, C.-D.; Terzis, A.; Chen, A.; Hutchison, J. E.; Clark, M. R.; Wignall, G.; Londono, J. D.; Superfine, R.; Falvo, M.; Johnson, C. S.; Samulski, E. T.; Murray, R. W. *J. Am. Chem. Soc*. **1995**, *117*, 12537.

(12) Hostetler, M. J.; Wingate, J. E.; Zhong, C.-J.; Harris, J. E.; Vachet, R. W.; Clark, M. R.; Londono, J. D.; Green, S. J.; Stokes, J. J.; Wignall, G. D.; Glish, G. L.; Porter, M. D.; Evans, N. D.; Murray, R. W. *Langmuir* **1998**, *14*, 17.

(13) Hostetler, M. J.; Stokes, J. J.; Murray, R. W. *Langmuir* **1996**, *12*, 3604.

(14) Hostetler, M. J.; Green, S. J.; Stokes, J. J.; Murray, R. W. *J. Am. Chem. Soc*. **1996**, *118*, 4212.

(15) Green, S. J.; Stokes, J. J.; Hostetler, M. J.; Pietron, J. J.; Murray, R. W. *J. Phys. Chem. B* **1997**, *101*, 2663.

(16) Ingram, R. S.; Hostetler, M. J.; Murray, R. W. *J. Am. Chem. Soc.* **1997**, *119*, 9175.

(17) Wuelfing, W. P.; Templeton, A. C.; Hostetler, M. J.; Murray, R. W. Manuscript in preparation.

(18) Templeton, A. C.; Hostetler, M. J.; Warmoth, E. K.; Krishnamurthy, V.; Hartshorn, C. M.; Forbes, M. D. E.; Murray, R. W. Submitted for publication.

S0002-7863(97)03863-8 CCC: $15.00
Published on Web 02/10/1998

reactivities of functional groups of the monolayers of Au clusters and, with a few exceptions, of functionalities on other types of monolayer-protected nanoparticles.[20,21] Alkanethiolate/Au MPCs can be both *polyhomo*-[14] and *polyheterofunctionalized*,[16] and are thereby potentially useful as large, poly-functionalized reagents. Realizing such usefulness, however, depends on understanding their various modes of reactivity. Are their reactions facile and comparable to those of analogous monofunctional monomers in solution, are their products easily isolated and characterized, and how do they depend on the surrounding monolayer structure? To what degrees are MPC reactions subject to steric, electrostatic, and dielectric medium effects? Do functional group reactivities on MPCs resemble those of ω-functionalized alkanethiolate monolayers on flat Au surfaces (2-D SAMs),[22] which are often difficult to characterize?

This investigation begins to address such questions. Understanding reactivity issues should prove valuable in engineering MPCs for applications such as nanoscale electronics,[23] chemical and biosensors,[24] drug delivery systems, and catalysis.[25] We are further interested in the concept of *polyheterofunctionalized*, working MPC "nanofactories" (supramolecular assemblies possessing reservoirs of centers with mutually supportive reactivities[16] capable of use as chemical reagents and catalysts, and analogous to biomolecules in mass and general morphology), and in using MPCs as metal-core scaffolds supporting more complex organic ligand structures including polymeric[17] and hyperbranched domains. MPCs with ω-functionalized alkanethiolate ligands in fact support a wide variety of reactions,[18] early groundwork platforming the "nanofactory" concept.

This paper addresses steric aspects of MPC reactivity, based on (a) S_N2 reactivity of ω-bromoalkanethiolate/Au MPCs with primary amines of graded steric bulk (*n*-propylamine, isopropylamine, *tert*-butylamine), under conditions of varied relative chain lengths of the ω-bromoalkanethiolate and of surrounding, unsubstituted alkanethiolate ligands, (b) the rate of cyanide-induced decomposition of gold cores protected by alkanethiolates of varied chain length and steric bulk, and (c) solution infrared spectroscopy exploring disorder characteristics of alkanethiolate ligand monolayers on Au MPCs. The steric environment of MPCs has important ramifications for the nanofactory MPC concept, since monolayer packing dictates the complexity of attainable ligand structure. Additionally, a sufficient understanding of the steric environment of reaction sites is a prelude to controlling access of substrates to reaction sites within designer diluent matrices, by incorporating noncovalent, stereochemical, hydrogen-bonding, or electrostatic interactions, analogous to those that govern enzyme−substrate complexes.

Experimental Section

Chemicals. $HAuCl_4 \cdot xH_2O$ was either purchased (Aldrich, 99.99%) or synthesized.[26] ω-Bromododecanethiol (BrC12SH), ω-bromooctanethiol (BrC8SH), and ω-bromopropanethiol (BrC3SH) were prepared according to the literature.[27] *n*-Propylamine (98%, Aldrich), isopropylamine (99%, Aldrich), *tert*-butylamine (99%, Aldrich), toluene, absolute ethanol, acetone, and tetrahydrofuran were used as received.

Spectroscopy. ^{1}H NMR spectra (in C_6D_6 or $CDCl_3$) were obtained with a Bruker AMX 200 MHz spectrometer. A line broadening factor of 1 Hz was used to improve S/N of MPC NMR data. Infrared absorbance spectra of clusters as thin films cast from solutions, as pressed KBr pellets, and in CCl_4 solutions were acquired with a Bio-Rad 6000 FTIR spectrometer.

MPC Synthesis. The MPCs used in this report were synthesized according to a modified literature procedure.[9,12] Briefly, toluene solutions containing a 3:1 ratio of alkanethiol to $AuCl_4^-$ were reduced at 0 °C with $NaBH_4$. Characterizations described elsewhere[12] show that this method produces an *average* Au core of 145 atoms covered by ca. 48−50 alkanethiolate chains. There is some dispersity of core size (and thus monolayer) in the samples used; present procedures[19c] for producing highly monodisperse materials are sufficiently tedious that studies of cluster chemical reactivity by core size are impractical.

ω-Bromo-Functionalized MPC Synthesis. Place exchange reactions were accomplished by a modification of the original procedure.[14] Specifically, the incoming ω-bromo-functionalized alkanethiols and ca. 2 mg of cluster/mL of the alkanethiolate/Au MPC were co-dissolved in toluene and stirred for 48−60 h at room temperature. After the solvent was removed under vacuum, the product was collected on a frit and washed serially with at least 150 mL of absolute ethanol and 100 mL of acetone. In such experiments, the extent of place-exchange (assumed to occur statistically over all clusters) depends on the starting feed ratio, i.e., the mole ratio of alkanethiolate chains originally on the MPCs to ω-bromo-functionalized alkanethiols placed in the exchange solution. The notation used throughout the report for the composition of the product MPCs is *a*:*b* C*X*:C*Y*Br, where *X* specifies the alkanethiolate chain length and *Y* the chain length of the incorporated ω-bromoalkanethiol (an equal amount of the original alkanethiolate, as thiol, is displaced[28]), and the number ratio a:b specifies the product mole ratio of *X* and *Y* chains in the cluster, as determined by the ^{1}H NMR ratio of methyl and $-CH_2Br$ resonances on *X* and *Y*, respectively. For example, a 1.5:1 C12:C12Br MPC product of exchange of ω-bromododecanethiol onto a dodecanethiol-protected cluster contains (on average) a mole ratio of the former to the latter chains of 1.5:1.

NMR of 1.5:1 C12:C12Br (in C_6D_6): δ (ppm) 0.98 (br, 4H), 1.42 (br, 44.5 H), 3.1 (br, 2H). NMR of 4:1 C12:C8Br (in C_6D_6): δ (ppm)

(19) (a) Badia, A.; Gao, W.; Singh, S.; Demers, L.; Cuccia, L.; Reven, L. *Langmuir* **1996**, *12*, 1262. (b) Badia, A.; Singh, S.; Demers, L.; Cuccia, L.; Brown, G. R.; Lennox, R. B. *Chem. Eur. J.* **1996**, *2*, 359. (c) Whetten, R. L.; Khoury, J. T.; Alvarez, M. M.; Murthy, S.; Vezmar, I.; Wang, Z. L.; Stephens, P. W.; Cleveland, C. L.; Luedtke, W. D.; Landman, U. *Adv. Mater.* **1996**, *8*, 428. (d) Ohara, P. C.; Leff, D. V.; Heath, J. R.; Gelbart, W. M. *Phys. Rev. Lett.* **1995**, *75*, 3466. (e) Luedtke, W. D.; Landman, U. *J. Phys. Chem.* **1996**, *100*, 13323. (f) Leff, D. V.; Brandt, L.; Heath, J. R. *Langmuir* **1996**, *12*, 4723. (g) Alvarez, M. M.; Khoury, J. T.; Schaaff, T. G.; Shafigullin, M. N.; Vezmar, I.; Whetten, R. L. *J. Phys. Chem. B* **1997**, *101*, 3706. (h) Cleveland, C. L.; Landman, U.; Shafigullin, M.; Stephens, P. W.; Whetten, R. L. *Z. Phys. D* **1997**, *40*, 503. (i) Vezmar, I.; Alvarez, M. M.; Khoury, J. T.; Salisbury, B. E.; Whetten, R. L. *Z. Phys. D* **1997**, *40*, 147. (j) Johnson, S. R.; Evans, S. D.; Mahon, S. W.; Ulman, A. *Langmuir* **1997**, *13*, 51. (k) Badia, A.; Cuccia, L.; Demers, L.; Morin, F.; Lennox, R. B. *J. Am. Chem. Soc.* **1997**, *119*, 2682. (l) Yonezawa, T.; Tominaga, T.; Richard, D. *J. Chem. Soc., Dalton Trans.* **1996**, 783. (m) Alvarez, M. M.; Khoury, J. T.; Schaaf, T. G.; Shafigullen, M.; Vezmar, I.; Whetten, R. L. *Chem. Phys. Lett.* **1997**, *266*, 91. (n) Yonezawa, T.; Sutoh, M.; Kunitake, T. *Chem. Lett.* **1997**, 619. (o) Buining, P. A.; Humbel, B. M.; Philipse, A. P.; Verkleij, A. J. *Langmuir* **1997**, *13*, 3921. (p) Andrews, R. P.; Bielefeld, J. D.; Henderson, J. I.; Janes, D. B.; Kolagunta, V. R.; Kubiak, C. P.; Mahoney, W. J.; Osifchin, R. G. *Science* **1996**, *273*, 1690. (q) Andrews, R. P.; Bein, T.; Dorogi, M.; Feng, S.; Henderson, J. I.; Kubiak, C. P.; Mahoney, W.; Osifchin, R. G.; Reifenberger, R. *Science* **1996**, *272*, 1323.

(20) Brust, M.; Fink, J.; Bethell, D.; Schriffrin, D. J.; Kiely, C. *J. Chem. Soc., Chem. Commun.* **1995**, 1655.

(21) (a) Noglik, H.; Pietro, W. J. *Chem. Mater.* **1994**, *6*, 1593. (b) Noglik, H.; Pietro, W. J. *Chem. Mater.* **1995**, *7*, 1333.

(22) (a) Ulman, A. *Chem. Rev.* **1996**, *96*, 1533. (b) Bishop, A. R.; Nuzzo, R. G. *Curr. Opin. Coll. Interface Sci.* **1996**, *1*, 127.

(23) (a) Schon, G.; Simon, U. *Colloid Polym. Sci.* **1995**, *273*, 101. (b) Schon, G.; Simon, U. *Colloid Polym. Sci.* **1995**, *273*, 202.

(24) Sampath, S.; Lev; O. *Adv. Mater.* **1997**, *9*, 410.

(25) Hoffman, A. J.; Mills, G.; Yee, H.; Hoffman, M. R. *J. Phys. Chem.* **1992**, *96*, 5546.

(26) (a) *Handbook of Preparative Inorganic Chemistry*; Brauer, G., Ed.; Academic Press: New York, 1965; p 1054. (b) Block, B. P. *Inorg. Syn.* **1953**, *4*, 14.

(27) Bain, C. D.; Troughton, E. B.; Tao, Y.; Evall, J.; Whitesides, G. M.; Nuzzo, R. G. *J. Am. Chem. Soc.* **1989**, *111*, 321.

(28) Displaced alkanethiolates reappear in solution as thiols. Dialkyl disulfides do not enter into place-exchange, but decomposition of clusters (thermal,[10c] cyanide-induced, I_2-induced) leads most generally to dialkyl disulfide products. Finally, the (initial rate) kinetics of place-exchange are first order in both cluster and in incoming alkanethiol concentration. (Hostetler, M. J.; Templeton, A. C.; Murray, R. W. Manuscript submitted for publication.)

0.98 (br, 13.7H), 1.42 (br, 92.5 H), 3.15 (br, 2 H). NMR of 10:1 C12:C3Br (in C_6D_6): δ (ppm) 0.98 (br, 3H), 1.42 (br, 19 H). Analogous NMR results were obtained for MPCs with other product mole ratios of alkanethiolate to ω-bromoalkanethiolate.

***ω*-Bromoalkanethiolate MPC Reactions with Primary Amines.** In a typical reaction, approximately 50 mg of ω-bromo-functionalized MPC was dissolved in 3.6×10^4 equiv of the selected (neat) primary amine. Following 3 h of stirring at room temperature, the amine was removed under vacuum and the solid washed with acetone (ethanol cannot be used; the starting material is insoluble in ethanol, but the product cluster is soluble) and dried. Reactions proceeded in ambient, with the exception of reaction with *tert*-butylamine (under N_2).

NMR of 1.5:1 C12:C12NHCH$_2$CH$_2$CH$_3$ (in C_6D_6): δ (ppm) 0.98 (br, 21.7 H), 1.42 (br, 125 H), 2.55 (br, 4 H). Spectra of other amine-reacted MPCs exhibited the same general features.

Product compositions resulting from reactions with primary amines were determined from changes in the ratios of terminal methyl to $-CH_2$-Br ^{1}H NMR resonances on the product clusters, from the ratios on the ω-bromo-functionalized starting materials, following background subtraction (see Supporting Information). Additionally, cluster reactions were qualitatively followed by using the CBr band in IR spectra.[29] Iodine-mediated cluster decomposition, which quantitatively liberates the MPC ligands as disulfides (vide infra), was used to confirm the ^{1}H NMR conversion and yield results, and gave identical results (within error).

12-Bromododecane (Monomer) Reaction with Propylamine. A 100 mg sample of 12-Bromododecane was dissolved in a 1050 M excess (68 mL) of *n*-propylamine and the mixture was stirred for 1 h at room temperature. Afterward, the solvent (amine) was removed under vacuum and the products characterized by ^{1}H NMR. NMR (in $CDCl_3$): δ (ppm) 0.82 (m, 16 H), 1.4 (m, 10 H), 1.7 (t, 4 H), 2.3 (q, 2 H), 2.5 (m, 6.6 H), 3.37 (t, 2 H).

MPC Reactions with Iodine. In a typical reaction, ca. 50 mg of the MPC dissolved in hexane was stirred with ca. 3 mg of iodine for 1 h. Following disulfide formation, which could be monitored by a change in solution color from dark brown to clear violet, the insoluble brown residue (actual identity of insoluble materials not yet determined) was removed and the sample rotovapped to dryness. NMR of I_2-decomposed 4:1 C12:C12Br product (in $CDCl_3$): δ (ppm) 0.85 (t, 4.4 H), 1.25 (m, 30H), 1.66 (m, 4H), 1.8 (m, 1.2H), 2.65 (t, 4H), 3.38 (t, 1.2 H). Other I_2-decomposed C12:CXBr product spectra were analogous. NMR of I_2-decomposed 1.5:1 C12:C12$-$NHCH(CH$_3$)$_2$ product (in $CDCl_3$): δ (ppm) 0.85 (t, 2.9H), 1.2$-$1.4 (m, 37H), 1.5$-$1.7 (m, 4.3H), 1.75$-$1.9 (m, 1.9 H), 2.45$-$2.6 (m, 0.26 H), 2.65 (t, 4H), 3.37 (t, 1.9 H). Other I_2-decomposed C12:C*X*NHR product spectra were analogous.

Kinetics of MPC Decomposition by NaCN. To a 3 mL solution of a Au MPC in THF (final concentrated $\sim$7.1 μM in cluster and 1.0 mM in Au) was added 0.5 mL of NaCN in H_2O (final concentrated $\sim$8.7 mM). After briefly agitating the solution, the decay in absorbance (at either 340 or 520 nm) was monitored over at least three reaction half-lives on an ATI UNICAM UV/vis spectrophotometer. The light brown cluster solution was decomposed into a mixture of colorless, slightly soluble AuCN complexes (this is assumed, actual identity of mixed materials not yet determined), dialkyl disulfides ($\sim$90% of the recovered organic matter), and alkyl cyanides (latter products were determined by ^{1}H NMR). The decomposition rate data were fit to a general first-order equation, $y = y' + ae^{-bx}$, where y' is the absorbance (i.e., loss of transmittance) due to light scattering by the finely suspended, inorganic reaction byproduct and was assumed to be constant.

Results and Discussion

S_N2 Reactions of ω-Bromo-Functionalized MPCs with Primary Amines. S_N2 displacement reactions on primary alkyl halides are well-known, high-yield routes[30] to other types of functional groups. S_N2 reactivity of ω-functionalized 2D-SAMs (self-assembled monolayers on flat surfaces) has been explored in several studies. Sukenik and co-worker[31] examined nucleophilic conversions of ω-bromo-functionalized alkyltrichlorosilanes on SiO_2 to azido- and thiocyanato-terminated surfaces, and their subsequent reduction to amino- and mercapto-terminated surfaces, respectively. Fryxell and co-workers[32] found nucleophilic substitution reactions on mixed monolayers of ω-bromo-functionalized alkyltrichlorosilanes on SiO_2 surfaces to be somewhat problematic; only with the strong nucleophile azide was complete reaction observed, and at a much slower rate than the analogous azide substitution on a dissolved primary alkyl halide monomer. In light of S_N2 mechanistic considerations (backside attack) and the well-known dense packing of 2-D SAMs on solid substrates,[33] it was concluded[32] that approach of incoming nucleophiles to the bromide groups is severely hindered by the surrounding monolayer hydrocarbon matrix.

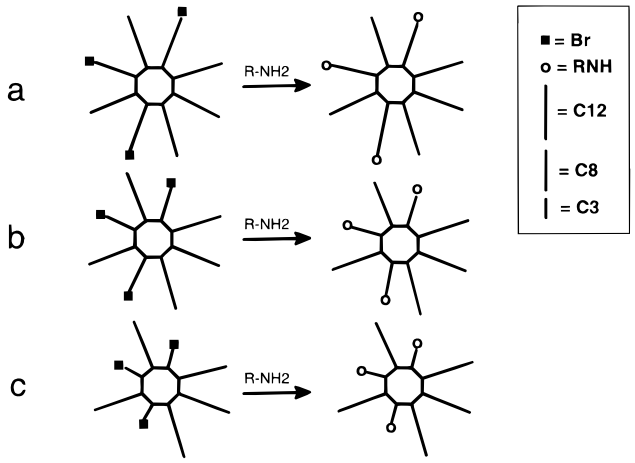

Figure 1. Schematic depicting the reaction of ω-bromo-functionalized MPCs with primary amines: (a) C12:C12Br, (b) C12:C8Br, and (c) C12:C3Br.

While we and others have pointed[10] to analogies between alkanethiolate monolayers on flat Au surfaces (2D-SAMs) and those on Au MPC cluster molecules ("3D-SAMs"), the two differ in that 3D-SAMs are attached to highly curved surfaces having a high Au surface defect density. It was accordingly not surprising to encounter in the present work a much more facile reactivity of ω-bromo-functionalized monolayers relative to that in the 2D-SAM reports.[31,32] The Figure 1 cartoon (roughly to scale) outlines a chain-length scheme for probing the steric environment of ω-bromoalkanethiolates on clusters. In Figure 1a, bromide resides on an alkanethiolate chain of length equal to the surrounding C12 alkanethiolates, whereas in Figure 1 parts b and c it resides on shorter (C8 and C3) chains and is putatively "submerged" within the cluster C12 alkanethiolate ligand shell.[34] The relative reactivities of these three mixed clusters with primary amines was explored by observing the extent of nucleophilic substitution occurring within fixed time periods and reaction conditions.

(29) IR spectroscopy was performed on all of the samples to follow the presence of bromide (C$-$Br, 563 cm^{-1}). Following transformation with amines, the IR spectra are informative on the presence of unreacted bromide ligand; however, characteristic secondary amine bands are not readily observed, which we explain on the basis of the presence of strong interfering alkanethiol bands and the general weakness of secondary amine bands.

(30) March, J. *Advanced Organic Chemistry;* Wiley: New York, 1985.

(31) Balachander, N.; Sukenik, C. *Langmuir* **1990**, *6*, 1621.

(32) Fryxell, G. E.; Rieke, P. C.; Wood, L. L.; Engelhard, M. H.; Williford, R. E.; Graff, G. L.; Campbell, A. A.; Wiacek, R. J.; Lee, L.; Halverson, A. *Langmuir* **1996**, *12*, 5064.

(33) Dubois, L. H.; Nuzzo, R. G. *Annu. Rev. Phys. Chem.* **1992**, *43*, 437.

(34) Evidence for the "submersion" of the functional groups comes from the observation that greater CH_2Br ^{1}H NMR peak broadening is observed for shorter connecting chains, in the order C12Br < C8Br << C3Br. For C3Br, the CH_2Br is broadened beyond recognition in the NMR spectra.

Table 1. Yield Data for Reactions of ω-bromo-functionalized MPCs with Primary Amines

MPC	ratio[a]	primary amine	% conversion[b]	conditions
C12:C12Br	19.9:1	*n*-propyl	95	3 h/RT
C12:C12Br	19.9:1	isopropyl	30	3 h/RT
C12:C12Br	19.9:1	*tert*-butyl	5	3 h/RT
C12:C12Br	19.9:1	*tert*-butyl	79	24 h/40 °C
C12:C12Br	4.5:1	*n*-propyl	95	3 h/RT
C12:C12Br	4.5:1	isopropyl	25	3 h/RT
C12:C12Br	4.5:1	*tert*-butyl	5	3 h/RT
C12:C12Br	4.5:1	*tert*-butyl	57[c]	24 h/40 °C
C12:C12Br	1.4:1	*n*-propyl	95	3 h/RT
C12:C12Br	1.4:1	isopropyl	10	3 h/RT
C12:C12Br	1.4:1	*tert*-butyl	5	3 h/RT
C12:C12Br	1.4:1	*tert*-butyl	84	24 h/40 °C
C12:C8Br	4.2:1	*n*-propyl	59	3 h/RT
C12:C8Br	4.2:1	isopropyl	10	3 h/RT
C12:C8Br	4.2:1	*tert*-butyl	5	3 h/RT
C12:C8Br	4.2:1	*n*-propyl	95	24 h/RT
C12:C8Br	4.2:1	*tert*-butyl	77	24 h/40 °C
C12:C3Br	10:1	*n*-propyl	5	3 h/RT
C12:C3Br	10:1	*n*-propyl	95	24 h/40 °C

[a] Determined from ratios of methyl and $-CH_2Br$ proton resonances, except for C12:C3Br which was determined by using I_2 decomposition (see Supporting Information). [b] Determined from changes in ratios of methyl and $-CH_2Br$ resonances in ^1H NMR spectra of reacted MPCs, and confirmed by the I_2-decomposition reaction, which gave identical results within measurement error (see Supporting Information). Results cited for the "buried" reactions are averages of three different measurements. In general, NMR integrations agreed within ca. 5%. [c] Anomalous data point (single experiment) that is inconsistent with other trends.

The upper part of Table 1 lists results for reaction a in Figure 1 of C12:C12Br MPCs with progressively more bulky primary amines—*n*-propyl, isopropyl, and *tert*-butyl. The order of reactivity, as expected, responds to steric bulk of the incoming amine nucleophile. For example, at room temperature, a 3 h reaction produced essentially complete reaction of *n*-propylamine, but very little of the *tert*-butylamine. However, under more vigorous conditions (24 h, 40 °C), even the bulky *tert*-butylamine nucleophile reacted to a substantial extent with the cluster-bound bromoalkanethiolate.

The lower part of Table 1 shows results for reactions b and c in Figure 1. The (3 h/RT) data for the C12:C8Br cluster reactivity with *n*-propyl and isopropylamines and for the C12:C3Br cluster with *n*-propylamine, compared to that of C12:C12Br clusters with the same amines, show clearly that reactivity is depressed by "submerging" the bromoalkanethiolate site within the monolayer of a dodecanethiolate MPC. The data again show, however, that nucleophilic substitution of even the "submerged" bromide sites can be fully realized for both *n*-propyl and *tert*-butylamine at longer reaction times and elevated temperatures.

Reaction a in Figure 1 was examined as a function of the average extent of loading of ω-bromoalkanethiolate on the MPCs (Table 1, top part). A 19.9:1 C12:C12Br cluster has an average population of 2.4 bromide sites per cluster, whereas a 1.4:1 C12:C12Br cluster has an average population of 20.8 bromide sites. The latter is nearly the limiting number of ω-bromoalkanethiolate sites that could be easily exchanged onto this size Au cluster (whether the limit is determined by steric constraints or a saturation of readily exchangeable sites is unclear). The differences in reactivity with loading are relatively minor, indicating that the steric environment for reaction of "*non*-submerged" bromoalkanethiolate sites with *n*-propylamine is favorable even when their numbers are large, i.e., an average individual 1.4:1 C12:C12Br cluster molecule undergoes 20 nucleophilic substitution reactions. (The effect of loading for "submerged" reaction sites was not investigated in the present study.)

The preceding result is consistent with a comparison of reactivity with *n*-propylamine between the "nonsubmerged" C12:C12Br MPC and that of a 12-bromododecane *monomer*, both under the same reaction conditions (1050-fold amine excess; 1 h/RT). The results showed that the "nonsubmerged" cluster bromo sites are nearly as reactive as those of the monomer (MPC, 50% substitution; monomer: 65% substitution), an observation in stark contrast to that on alkyltrichlorosilane-based 2D SAMs.[32] This comparison indicates that *the steric environment of "nonsubmerged" functional groups on MPCs is not strongly different from that of monomers in solution.* In this respect, any analogy between 2D-SAMs and cluster 3D-SAMs fails; the two kinds of monolayers exhibit major differences in terms of S_N2 reaction chemistry.

The Table 1 results show that the sensitivity of nucleophilic substitution reactivity to nucleophile bulkiness increases when the reaction center is submerged within a surrounding alkanethiolate monolayer. Both submersion and bulk effects are reasonably interpreted in terms of steric inhibition of S_N2 backside attack. The results suggest at least the following about S_N2 reactions on MPCs of the size considered here: (a) that the *entire* ligand structure of such molecules is to some degree open to attack, because of substantial chain mobility and a relatively open, uncompacted monolayer structure, and/or (b) that an exceptional reactivity preference is imparted to *certain* ligands as a result of their location on the gold core. For example, ω-bromoalkanethiolates that have been exchanged onto Au core vertexes and edges ("defect sites") may be more receptive to backside attack than those on terrace-like Au core sites, due to a more spacious ligand environment resulting from the curvature of the surface. Differentiation of these two possibilities rests on an analysis (an interesting but future[35] research topic) of alkanethiolate site location (and possible mobility thereof) on mixed-monolayer Au MPCs.

Two mechanistic scenarios exist for primary amine reactions with the MPC ω-bromoalkanethiolate ligands: the Au−S bond remains intact during reaction, or the ligand becomes partially or fully dissociated from the gold core (such as to a cage-like complex that, following nucleophilic displacement, collapses to re-form the Au−S bond). The available evidence strongly favors the former mechanism. (*i*) Whereas questions remain about whether place-exchange reactions on 2D SAMs of alkanethiolates on gold occur by associative or dissociative pathways,[36] our results show that place-exchange reactions on Au MPCs proceed via an associative pathway in which an incoming alkanethiol displaces one bound alkanethiolate ligand.[28] (*ii*) Considering that molecules other than alkanethiols might promote place-exchange reactions, primary amines were tested and found not to facilitate or catalyze them.[37] (*iii*) Significant evidence is available from the reactivity results (vide supra). For example, Au−S bond dissociation and cage complex

(35) Analysis of separated disulfides should provide insights as to ligand adjacency. Thus, islanding of a functionalized alkanethiolate could be detected by comparing the measured distribution of the disulfide products (i.e., R′SSR, RSSR, R′SSR′) with that expected for a random distribution of neighbors. Implementation of this technique is in progress.

(36) (a) Schlenoff, J. B.; Li, M.; Ly, H. *J. Am. Chem. Soc*. **1995**, *117*, 12528. (b) Collard, D. M.; Fox, M. A. *Langmuir* **1991**, *7*, 1192. (c) Hickman, J. J.; Ofer, D.; Zou, C.; Wrighton, M. S.; Laibinis, P. E.; Whitesides, G. M. *J. Am. Chem. Soc*. **1991**, *113*, 1128.

(37) Cluster place-exchange reactions (nonlimiting coverages) produced essentially the same product ratios in the presence of amine.

formation preceding nucleophilic attack should lessen or remove any reactivity differences between the "nonsubmerged" C12:C12Br and the "submerged" C12:C8Br and C12:C3Br MPCs, especially since the *C3Br* ligand *should* be *most likely* to dissociate from the core in relief of strain in the tightly packed region near the gold core. However, nucleophilic reactions occur facilely on C12:C12Br MPCs, but only under vigorous conditions on the C12:C3Br cluster, which is inconsistent with dissociation. (*iv*) Highly loaded clusters would exhibit enhanced reactivity were the reaction dissociative, but no such difference was observed even at higher loading of ω-bromo-functionalized ligands. (*v*) The substantial thermal stabilities[10] of the clusters and their stability to both extensive washings and solvation/reisolation with various organic solvents makes facile thiolate ligand desorption/reabsorption an unlikely process. Considering the collective weight of the evidence, we believe that the S_N2 reactions explored in this study occur predominantly on ligands with intact Au−S bonds.

Analysis of S_N2 Reaction Products Using Iodine Chemistry. Significant points to consider in the analysis of products of amine reactions with the ω-bromo-functional groups on MPCs are the following: (*a*) amines can adsorb on gold,[38] giving a potential alternative explanation of loss of the C−Br infrared band in the MPC product without nucleophilic substitution having actually occurred; (*b*) the possibility exists for the formation of tertiary as well as secondary amine products (as occurs on monomer reactants)—this would be difficult to detect given the broadened nature of MPC NMR spectra;[11] and (*c*) the methyl/$-CH_2Br$ resonance in the ^1H NMR spectra must be interpreted through differences in their ratios before and after reaction with amines, to obtain reaction yield data (see Supporting Information). These issues and related uncertainties were resolved by decomposing the MPCs by reaction with I_2, which quantitatively liberates the alkanethiolate monolayer as dialkyl disulfide compounds[39a] with intact end-group functionalities. Thus, upon isolation, the sharp ^1H NMR resonances of the disulfides provide both the identity of all of the former alkanethiolate ligands and their relative populations.

As noted in the Experimental Section, place-exchanged cluster $CH_3/-CH_2Br$ ratios obtained by ^1H NMR of the clusters and by the above methodology were in agreement. This comparison was carried out for all reaction yield results reported in Table 1. Additionally, NMR spectra in the I_2 decomposition studies indicate formation of only secondary amines; no tertiary amine formation was detected even at higher bromide coverages. This is in marked contrast to experiments on alkyl bromide monomers dissolved in solution, where ca. 14% of all groups reacted further to form tertiary amines. Intramolecular tertiary amine formation on the MPCs would be a ring-forming step requiring relatively close terminal bromo sites and is apparently inhibited under the reaction conditions employed (large excess).

Using the I_2-decomposition reaction to examine the protective effects of the monolayer ligand shell proved difficult.[39b] Such studies were, however, successful for NaCN chemistry which is described next.

NaCN-Induced Decomposition of MPCs. Work on alkanethiolate/gold 2D SAMs has shown[40−42] that cyanide causes the dissociation of the monolayer with concomitant etching of the gold underlayer. The rate of decomposition can be correlated to the extent to which a particular alkanethiolate monolayer provides a protective barrier to the gold surface.

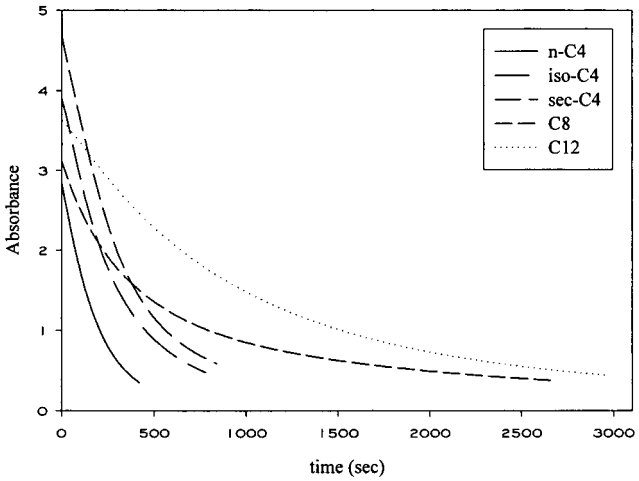

Figure 2. Plots representing a first-order fit of absorbance data for the reaction of NaCN with the gold clusters over a wide range of protecting ligand sizes and chain lengths.

Table 2. Rate Constants for the Decomposition of Au MPCs with NaCN[a]

cluster protecting group	k_1, s^{-1}	k_2, $M^{-1}\ s^{-1}$
n-C4[b]	$(5.16 \pm 0.09) \times 10^{-3}$	$(8.9 \pm 0.3) \times 10^{-1}$
iso-C4	$(3.62 \pm 0.06) \times 10^{-3}$	$(6.2 \pm 0.2) \times 10^{-1}$
sec-C4	$(3.09 \pm 0.05) \times 10^{-3}$	$(5.3 \pm 0.2) \times 10^{-1}$
C6	$(3.00 \pm 0.01) \times 10^{-3}$	$(5.2 \pm 0.2) \times 10^{-1}$
C8	$(1.93 \pm 0.02) \times 10^{-3}$	$(3.3 \pm 0.1) \times 10^{-1}$
C8[c]	$(2.98 \pm 0.02) \times 10^{-3}$	$(3.4 \pm 0.1) \times 10^{-1}$
C8[d]	$(5.41 \pm 0.02) \times 10^{-3}$	$(3.7 \pm 0.1) \times 10^{-1}$
C10	$(1.20 \pm 0.01) \times 10^{-3}$	$(2.1 \pm 0.1) \times 10^{-1}$
C12	$(1.03 \pm 0.02) \times 10^{-3}$	$(1.8 \pm 0.1) \times 10^{-1}$
C16[b]	$(1.39 \pm 0.01) \times 10^{-3}$	$(1.6 \pm 0.1) \times 10^{-1}$

[a] Rate constants were derived from data collected over at least 3 half-lives. [b] Concentration of NaCN was 5.8 mM unless otherwise stated. [c] [NaCN] = 8.7 mM. [d] [NaCN] = 14.6 mM.

Our experiments show that dark brown alkanethiolate/Au MPC solutions are converted by NaCN in 6:1 THF/H_2O to a mixture of colorless Au compounds, liberating the monolayer as (mostly) soluble dialkyl disulfides. The progress of the decomposition reaction can be monitored with UV/vis spectroscopy (Experimental Section). Figure 2 shows a first-order fit of the absorbance data (see Experimental Section) for the reaction of NaCN with the gold clusters over a range of protecting alkanethiolate chain lengths. Importantly, the reaction is first order (see C8 results in Table 2) in both [NaCN] and [cluster], and the reaction rates are unchanged by the amount of oxygen present. Table 2 gives both pseudo-first-order (in NaCN) and second-order rate constants (data collected and fit over at least 3 half-lives) for the reactions.

The results show, as reasonably expected, that decomposition is most rapid for clusters protected by short (butanethiolate) ligands, and slows for longer chain lengths (Table 2). For example, the octanethiolate-protected MPC decomposes 2.5 times more slowly than the butanethiolate MPC, implying that

(38) Leff, D. V.; Brandt, L.; Heath, J. R. *Langmuir* **1996**, *12*, 4723.

(39) (a) For example, decomposition by I_2 of a 250 mg sample of C12 MPC (alkanethiolate ligand content 65 mg) produced 63 mg of disulfide (a quantitative conversion) following removal of insoluble material and unreacted iodine. Spectrophotometric analysis of starting and final solutions for I_2 concentration indicates that the decomposition reaction stoichiometry is 3:1 alkanethiolate:I_2. (b) The high background absorbance/scattering of the insoluble (presumably Au-containing) reaction product prevented spectrophotometric analysis of the reaction kinetics.

(40) Kumar, A.; Whitesides, G. M. *Appl. Phys. Lett.* **1993**, *63*, 2002.

(41) Weisbecker, C. S.; Merritt, M. V.; Whitesides, G. M. *Langmuir* **1996**, *12*, 3763.

(42) Gorman, C. B.; Biebuyck, H. A.; Whitesides, G. M. *Chem. Mater.* **1995**, *7*, 252.

Table 3. Infrared Spectroscopic Data for Alkanethiolate-Protected Clusters

chain length	KBr pellet[a,b]	dropcast film[b]	solution[b,c]	2D-SAM[b,d]
C4	2859, 2924	2859, 2924	2861, 2931	n/a
C8	2850, 2920	2852, 2922	2853, 2925	2852, 2921
C12	2850, 2920	2852, 2922	2853, 2925	2851, 2929

[a] See ref 13. [b] d^+, d^-; in cm^{-1}. [c] In CCl_4. [d] See ref 43c.

the octanethiolate ligands are more effective at preventing NaCN from approaching the Au/thiolate interface. It seems reasonable to conclude that the C8 monolayer provides a greater steric barrier and a thicker hydrophobic shell which resists ionic penetration.

A fascinating aspect of these experiments is that all MPC monolayer barriers of ≥C10 provide essentially the same degree of protection to NaCN-induced decomposition. This result is distinct from that observed with 2D-SAM systems,[22] but agrees with studies[41] of 38 nm gold colloids protected with $HS(CH_2)_n$-CO_2H monolayers. The results are consistent with a picture[12] of a MPC gold core surrounded by a densely packed alkane region, which is further surrounded by a less compact alkane region (i.e., there is a gradient of chain packing density, and the density nearest the Au/thiolate interface is unaffected by further chain length increase).

Table 2 also includes pseudo-first-order rate constants for decomposition of the isobutylthiolate and *sec*-butylthiolate MPCs. The *tert*-butyl protected cluster was not considered due to the insolubility of the prepared material. The branched monolayers provided substantially more protection, with the general stability trend *sec*-C4 > *iso*-C4 > *n*-C4. Interestingly, the *sec*-C4 MPC had stability ca. equal to that of the *n*-C6 MPC, indicating that one way in which protecting ligands can prevent access to the gold core is by forming a more compact, space-demanding layer.

Infrared Spectroscopy. Infrared spectroscopy is a classic technique[43−45] for investigating the conformation of alkane chains on 2-D SAMS. For adsorbed alkanethiolate ligands, the positions of the d^+ (CH_2 symmetric stretching vibration) and the d^- (CH_2 antisymmetric stretching vibration) bands are highly sensitive indicators of MPC chain conformation.[13] Table 3 shows positions of these bands for the alkanethiolate/Au MPCs as a function of chain length in the solid state as KBr pellets and as drop-cast films, in CCl_4 solution, and for the corresponding alkanethiolates as a 2D SAM on a flat gold surface.[43c] For comparison, d^+,d^- bands which are valuable metrics for understanding their range of values are those for crystalline polyethylene (2850, 2920 cm^{-1}) and liquid heptane (2855, 2924 cm^{-1}).[44]

As can be seen, when the C8 and C10 MPCs are pressed into a KBr pellet, the chain ordering is similar to that of the same alkanethiolate chains in 2D-SAMs. Such highly ordered systems have their methylene groups in an all-trans configuration, like that of crystalline polyethylene.[13] The ordering is slightly less in MPC dropcast films (which have not been subjected to pressure). However, in solution, the alkanethiolate chains on the MPC become highly disordered, and despite being bound by one end to a gold core, they are quite liquidlike.

We currently assume that the alkanethiolate ligands do not freely migrate across the gold core surface,[35] and as in our analysis of ^{13}C NMR on dissolved MPCs,[11] our picture of these ligands is of a molecular fragment held in place at one end, but rapidly gyrating about at the other. This molecular mobility is probably associated with the strongly curved Au core surface, for instance, for a C12 monolayer on a 145 atom gold core, the packing density near the Au surface would be 9-fold that for fully extended alkyl methyl groups. An apparent consequence of high chain end mobility in solution is that measured hydrodynamic radii of the Au MPCs are less than those of simple addition of the gold core radius and fully extended alkanethiolate chain length (diffusion-order spectroscopy[11] and rotating disk voltammetry[14,15]).

Conclusions

The present results are a first step toward exploiting the reactivities of alkanethiolate/Au nanoparticles. Key findings regarding the steric environment of their monolayer ligand shells are as follows:

(*i*) S_N2 reactions of *ω*-bromo-functionalized MPCs indicate that selectivity and rate of reaction are jointly controlled by the steric bulk of the incoming nucleophile and the spatial placement of the *ω*-bromo- reaction center within surrounding alkanethiolate diluent chains. The reaction retardation observed for submerged *ω*-bromo- groups may prove to be a useful effect in designing cluster materials that perform substrate-selective transformations.

(*ii*) *ω*-Bromo-functionalized MPCs have reactivity comparable to that of primary alkyl halide monomers (RBr). This result suggests that the utility of S_N2 chemistry on MPCs will not be significantly reduced by the matrix steric hindrance found[32] for 2D SAMs.

(*iii*) The rate of NaCN-induced decomposition decreases with increasing alkanethiolate chain length and steric bulk. This effect levels off for chain lengths greater than C10. Understanding cluster-core decomposition is of course relevant to defining the limitations on synthetic reagents that can be employed in reactions of functionalized clusters.

(*iv*) Infrared spectroscopic studies indicate that MPC alkanethiol ligands have a disorder in cluster solutions that approaches that of liquid alkanes. This result is consistent with the facile solution-phase S_N2 reactivity observed, and further suggests that substantially more complex ligand structures can be accommodated on MPCs.

In sum, the results are consistent with a highly vagile MPC ligand environment in which chain packing density decreases at progressively increasing distances from the gold core, and provides encouraging evidence that gold MPCs have potential as massively polyfunctional chemical reagents.

Acknowledgment. This research was supported in part by grants from the National Science Foundation and the Office of Naval Research. We also acknowledge helpful discussions with Professors M. R. Gagné and M. T. Crimmins of the Department of Chemistry at UNC-CH.

Supporting Information Available: Example NMR spectra of *ω*-bromo-functionalized MPCs, both before and after reaction with *n*-propylamine (2 pages, print/PDF). See any current masthead page for ordering information and Web access instructions.

JA973863+

(43) (a) Nuzzo, R. G.; Fusco, F. A.; Allara, D. L. *J. Am. Chem. Soc.* **1987**, *109*, 2358. (b) Nuzzo, R. G.; Dubois, L. H.; Allara, D. L. *J. Am. Chem. Soc.* **1990**, *112*, 558. (c) Porter, M. D.; Bright, T. B.; Allara, D. L.; Chidsey, C. E. D. *J. Am. Chem. Soc.* **1987**, *109*, 3559.

(44) (a) Snyder, R. G.; Strauss, H. L.; Elliger, C. A. *J. Phys. Chem.* **1982**, *86*, 5145. (b) Snyder, R. G.; Maroncelli, M.; Strauss, H. L.; Hallmark, V. M. *J. Phys. Chem.* **1986**, *90*, 5623.

(45) (a) Hayashi, M.; Shiro, Y.; Murata, H. *Bull. Chem. Soc. Jpn.* **1966**, *39*, 112. (b) Bryant, M. A.; Pemberton, J. E. *J. Am. Chem. Soc.* **1991**, *113*, 8284.